Journal Name RSCPublishing

COMMUNICATION

Functional Graphene Springs for Responsive Actuation

Cite this: DOI: 10.1039/x0xx00000x

Huhu Cheng,[a] Yuan Liang,[a] Fei Zhao,[a] Yue Hu,[a] Zelin Dong,[a] Lan Jiang,[b] and Liangti Qu*[a]

Received 00th January 2012,
Accepted 00th January 2012

DOI: 10.1039/x0xx00000x

www.rsc.org/

A new type of graphene fiber spring (GFS) has been demonstrated to possess a large elongation of up to 480% with a stable elasticity coefficient for 100000 times of stretch. Remarkably, GFS performs reversibly stretchable actuationunder electrostatic effects, and responds to the applied magnetic field for development of novel magnetostriction switches and actuators once functionalized with magnetic nanocomponents.

Graphene fiber (GF) has been well recognized because it integrates the remarkable properties of individual graphene sheets into the useful, macroscopic ensembles.[1–3] In comparison with carbon nanotube-based fibers,[4] GFs possess the unique advantages over conventional carbon fibers such as low cost, light weight, shapeability and ease of functionalization.[1–3,5,6] Achievements have been done to fabricate GFs by directly assembling graphene oxide (GO) through a dimension-confined hydrothermal strategy[1] and a large-scale spinning method[2,3,5–7] as demonstrated by us and other groups.

GFs have indeed provided a new material platform for developing a variety of unconventional fiber-based devices. For examples, the novel type of actuators based on GF/polypyrrole (PPy) bilayer structure[8] and graphene/graphene oxide (G/GO) asymmetric fibers have displayed complex, well-confined, predetermined motion and deformation,[7] which could be applied as multi-armed tweezers or amazing walking robots.[7,8] By reconstructing the intrinsic configuration of graphenes within the fiber body, a moisture-driven rotational motor is also achieved,[9] which enables the reversible torsional rotation with a maximum rotation rate of up to 5190 rotations min^{-1}. This provides the chance to develop the promising humidity-triggered electric generators that produce power using mechanical work induced by the variation of ambient moisture. Interestingly, based on the hollow GF functionalized site-specifically, a self-powered grapheme micromachine can move in aqueous medium.[5] In addition to these mentioned above, other impressive examples include the GF-based flexible dye-sensitized photovoltaic cells[10] and all-solid-state fiber supercapacitors.[11]

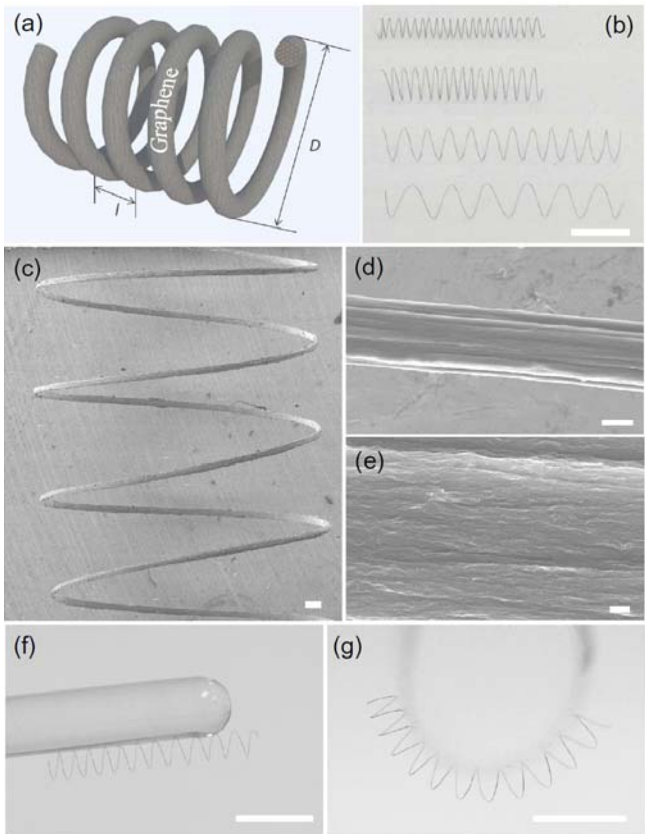

Fig. 1 (a) Scheme of a GFS.*D* is the diameter of GFS. *l* is the distance between loops. (b) Photo of GFSs with tunable diameters and loop distances. (c) SEM images of a GFS. (d) The surface of GFS and (e) the enlarged view of (d). (f, g) Photos of GFS attracted by the glass rod and the bent plastic film charged electrostatically. Scale bars: b, 5 mm; c, 100 μm; d, 10 μm; e, 1 μm; f, g, 1 cm.

Spring is an elastic device that can control the mechanical movement, ease the shock/vibration, conserve energy and measure the force, which thus is important for mechanical and electronic industry. It can conformably deform under loading process related with the transfer of mechanical energy and/or kinetic energy to the energy of deformation. Once unloaded, the spring recovers to its initial state and accordingly the deformation energy is converted to the mechanical energy and/or kinetic energy. Most of the commercial springs are made of metals. In contrast, carbon-based springs are less developed probably due to the low elasticity of the common carbon materials, although they possess the remarkable properties of light weight, tolerance to the harsh conditions plus high thermal and electrical conductivity.

Herein, we demonstrate a new type of unique graphenefiber spring (GFS). It possesses a large elongation of up to 480% while sustaining a small tensile strength of only 0.12 mN. Remarkably, the GFS presents a stable coefficient of elasticity even for one hundred thousand times of stretch with a strain of 300%. Particularly important, the GFS can behave elastically in an electrically or magnetically controllable fashion. Under electrostatic effects, the graphene spring exhibits outstanding performance as a reversibly stretchable actuator with a 210% expansion. Functionalized with magnetic nanocomponents, graphene spring can be actuated in response to the applied magnetic field, allowing for development of novel magnetostriction switches and actuators.

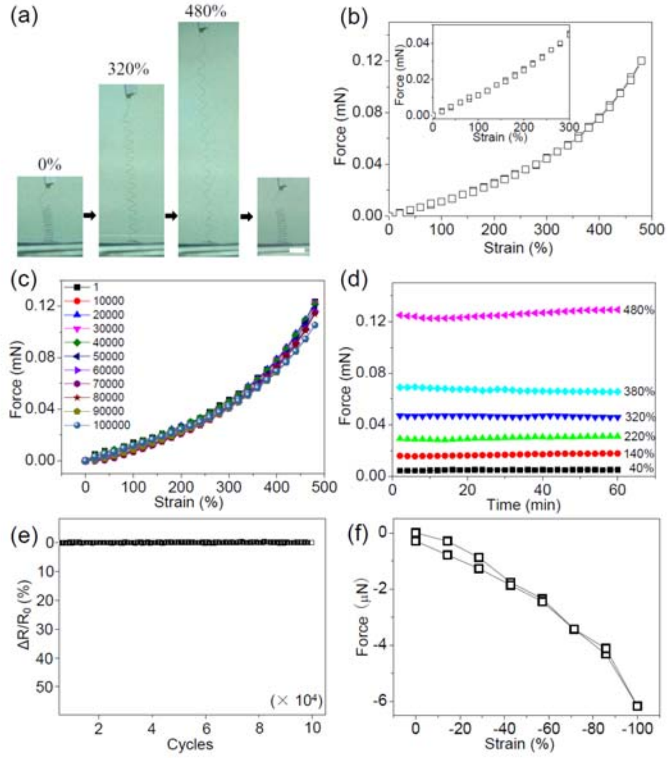

Fig.2 (a) Photos of the GFS was stretched to the strain of 0%, 320%, 480% and recovered to the original state (from left to right), respectively. Scale bars: 5 mm. (b) Force-strain curve of GFS during stretching process (D = 3mm, l = 1mm). (c) Force-strain curves of 100000 stretch cycles. (d) Recorded force relaxation (normalized to initial force value) by maintaining the GFS at strains of 40%, 140%, 220%, 320%, 380% and 480%, respectively. (e) The relative electrical resistance change ($\Delta R/R_0$) during cyclic testing. ΔR stands for the electrical resistance change and R_0 is the initial resistance. (f) Force-strain curve of GFS under the compression-release process.

The graphene spring was readily fabricated by wrapping the as-prepared wet GF around the cylindrical objects such as glass bar (Figure S1), followed by annealing it under 500°C to maintain the structure stability. As shown in Figure 1a and 1b, GFSs with different diameters (D) and loop distance (l) can be easily achieved by varying the internal cylinders and controlling the winding density of GFs. Although the shape of GF have changed from line type into a spiral structure, scanning electron microscopy (SEM) images of the GFS reveal that the surface is closely wrapped by the grapheme sheets (Figure 1c–e) and the fiber body is full of uniform graphene sheets arranged along the axial direction (Figure S2) similar to the common GF.[1] X-ray diffraction (XRD) patterns and X-ray photoelectron spectroscopy (XPS) results (Figure S3) also indicated the GO have been fully converted into grapheme sheets in GFS. The GFS is extremely light and mechanically flexible, which can be easily attracted by glass rod (Figure 1f) and plastic film with deformation (Figure 1g) once static electricity is induced on them by slight friction.

The spring sample of 20 µm GF has a diameter of about 3 mm and an average loop distance of 1 mm. The loops of graphene spring gradually expand with the increase of tension but without any structural breakage during the cycling test, indicating its mechanical ductibility.

The graphene spring has a large tensile strain of up to 480% (Figure 2b), and it can fully recover to its original state (Figure 2a) due to the excellent mechanical flexibility of GFs.[1] The cyclic test of graphene spring for one hundred thousand times with a strain of 480% displays almost unchanged strain-force curves (Figure 2c), demonstrating the long-term stability of the graphene spring. Accordingly, SEM image of graphene spring after mechanical testing (Figure S4) showed no obvious changes of the assembled graphene structures of the fiber.

The strain showed nearly linear relationship versus the applied force within the strain region of 300% (Figure 2b, inset). The elasticity coefficient (k) can be estimated by the followingequation:[12]

$$k = Gd^4/64r^3N$$

Where d is the diameter of the GF in GFS, G is the shear modulus ($G = E/2(1+v)$, where E is the graphene fiber's Young's modulus, v is Poisson's ratio), r is the radius of the loop and N is the number of the loops in the measured GFS sample.[12, 13] The Young's modulus of GF can be obtained from its stress-strain curve (Figure S5). If we adopted a conventional Poisson's ratio of 0.3, a shear modulus of G = 8 GPa and $k = 4.6\times10^{-4}$ N m^{-1} are obtained. This spring constant value is consistent with that obtained from slope curve in the inset of Figure 2b ($k = 6.8\times10^{-4}$), which is close to that of DNA molecules (10^{-5} N m^{-1})[14, 15] and orders of magnitude lower than that of some inorganic nanohelicies (10^{-2} to 10^{-3} N m^{-1})[16, 17] although GFS is a macroscopically assembled structure. After 800°C annealing processing, the GFS maintain a stable elasticity coefficient (Figure S6). Due to the low elasticity coefficient, GFS can be easily attracted and stretched by a static electricity-charged glass rod (Figure S7). The strain response of GFS is much more efficient than the conventional metal (e.g., copper) spring (Figure S8). With the low-stiffness and high-strain capability, the GFS would be used as sensitive tiny force sensor for microscopic displacement measurement.[16, 17]

To investigate its tolerance to fatigue, we have fixed the GFS at certain elongations and recorded the evolution of tensile stress over a period of 60 minutes (Figure 2d). It is observed that the applied forces for each stretching states remain stable, indicating the high anti-fatigue feature of the GFS. In fact, the mechanical properties of GFS can be tuned easily by controlling the loop density and spring diameter of GFS (Figure S9).

The GFS has a four-probe electrical conductivity of ~10 S/cm at room temperature, which is similar to the GF we have reported.[1] After one hundred thousand cycles of stretching test with a strain of 480%, the almost unchanged electrical resistance indicated the excellent electrical stability of GFS (Figure 2e), suggesting the great potential applications in stretchable circuits and flexible devices.

The compression performance of GFS was also tested with the applied load (Figure 2f). The GFS becomes short and can recover to its original length when the load was removed. Thecorresponding energy absorption values can be calculated by the integral of area under each curve.[18] The energy absorption density of GFS is about 1.04×10^{-4} J/g, which is much lower than of steel springs (0.14 kJ/kg),[19–21] implying the potential for tiny elastic energy storage.[22]

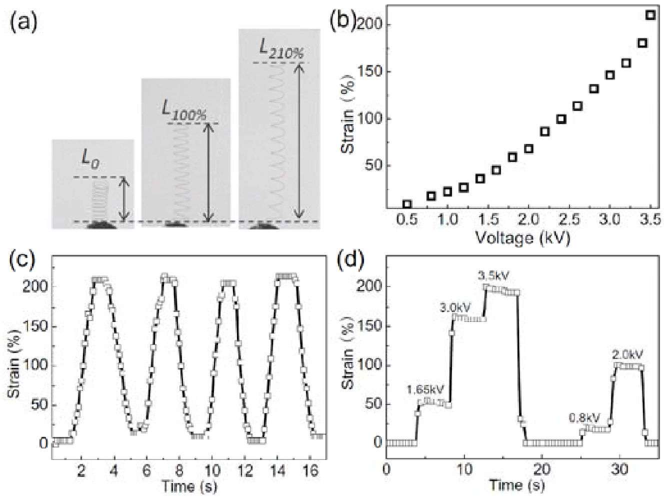

Fig.3 (a) Photos of GFS showing the strain response of 0%, 100% and 210% at applied voltage of 0, 2.2 and 3.5 kV, respectively. (b) Strain response as a function of applied voltages to GFS. (c) Strain changes with the on/off applied voltage of 3.5 kV. (d) Discretionarily controlled strain response of GFS by applying the certain voltage.

The high strain response of GFS allows the development of large displacement actuators.[23] Actuation behavior could be induced by an electrostatic field. For this purpose, an electrostatic generator was connected to the GFS. When the applied voltage rises from 0 to 3.5kV, GFS can controllably elongate with a strain of up to ca. 210% (Figure 3a and b) due to the repulsive force between the charged loops of GFS. This shape change is similar with the electrostatically actuated carbon nanotube aerogel sheets (220%).[24]The reversible expansion process of GFS has a voltage-dependent strain response (Fig 3b and c), and the length change is approximately linear with the applied voltage. Therefore, we can discretionarily control the length of GFS by applying the certain voltage (Figure 3d). Remarkably, within a very short time of about 1 second, the GFS can stretch 210% at applied voltage and return to its initial state upon removal of voltage (Figure 3c and Movie S1). The actuation rate is ca. 210%/s, which is much faster than the maximum 20 %/s achieved for the electrically driven carbon nanotube yarn or sheet actuators and the maximum rate of 50%/s for natural muscle.[25]

The GFS can be further functionalized by combination with other stimulus-responsive components. As an example, magnetic GFS has been fabricated by introduction of Fe_3O_4 nanoparticles into the GFS (Figure S10). As shown in Figure 4a, the Fe_3O_4 functional GFS (Fe_3O_4-GFS) can act as magnetically driven actuator by applying an external magnetic field. The GFS will contract when a magnet is placed below it, and reversely the GFS was stretched once the magnet is above it.

The excellent magnetically driven stretchable actuation of GFS plus its electric conductivity (~8 S/cm) enables to fabricate the new-type of magnetic switch. As a proof-of-concept prototype shown in Figure 4b and c, the switch was built by a simple circuit including a battery, a light emitting diode (LED) and two plane electrodes with a magnetism-responsive GFS connected with one of them (Figure S11). When the magnetic field is on, the GFS will contract and disconnect the circuit, which hence turn off the LED. Upon removal of magnetic field, the GFS can recover to the original position making connection of the two electrodes again and turn on the light (Movie S2). In principle, the electric conductivity could be further improved by increasing the annealing temperature (Figure S12).

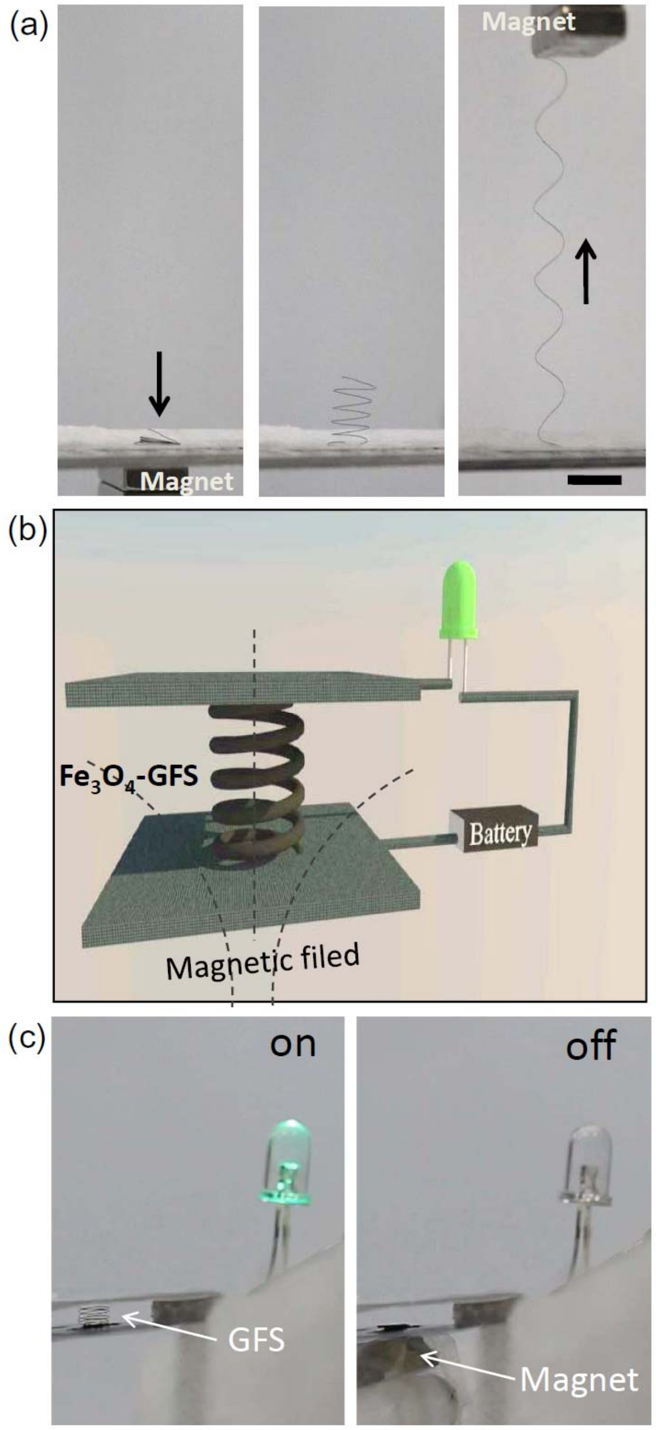

Fig. 4 (a) Photos of Fe_3O_4-GFS of original state (meddle), contraction state (left) and elongation state (right) driven by a magnet. Scale bar: 5mm. (b) Scheme of Fe_3O_4-GFS switch in a circuit, where GFS responds to the

magnetic field to maintain the "close" and "open" states. (c) The LED in "on" and "off" states as the circuit is connected and disconnected under the applied magnetic field. The GFS diameter is 3 mm.

Conclusions

In conclusion, we have fabricated a new type of graphene spring with a large elongation of up to 480%. The GFS presents a stable coefficient of elasticity even for one hundred thousand times with a strain of 300%. On the basis of the low-stiffness and high-strain capability, the graphene spring presents outstanding performance as a reversibly stretchable actuator with a 210% expansion under electrostatic effects. Beyond this, functionalized graphene spring can be actuated in response to the applied magnetic field, allowing for development of novel magnetostriction switches, actuators and other interesting applications.

Acknowledgements

We thank the financial support from the 973 program of China (2011CB013000) and NSFC (21325415, 21174019, and 51161120361), Fok Ying Tong Education Foundation (no. 131043), and 111 Project 807012.

Notes and references

[a] *Key Laboratory of Cluster Science, Ministry of Education of China; Beijing Key Laboratory of Photoelectronic/Electrophotonic Conversion Materials, School of Chemistry, Beijing Institute of Technology, Beijing 100081, P. R. China. Fax: 8610 68918608; Tel: 8610 68918608; E-mail: lqu@bit.edu.cn*
[b] *Laser Micro-/Nano-Fabrication Laboratory, School of Mechanical Engineering, Beijing Institute of Technology, Beijing 100081, P. R. China*

†Electronic Supplementary Information (ESI) available: [Fabrication and characterizations of GFS]. See DOI: 10.1039/b000000x/

1 Z. L. Dong, C. C. Jiang, H. H. Cheng, Y. Zhao, G. Q. Shi, L. Jiang, L. T. Qu, *Adv. Mater.*,**2012**, *24*, 1856–1861.
2 Z. Xu, C. Gao, *Nat. Commun.*, **2011**, *2*, 571.
3 H. P. Cong, X.C. Ren, P. Wang, S. H. Yu, *Sci. Rep.*, **2012**, *2*, 613.
4 M. Zhang, K. R. Atkinson, R. H. Baughman, *Science*, **2004**, *306*, 1358–1361.
5 C. G. Hu, Y. Zhao, H. H. Cheng, Y. Wang, Z. L. Dong, C. C. Jiang, X. Q. Zhai, L. Jiang, L. T. Qu, *Nano Lett.*,**2012**, *12*, 5879–5884.
6 Y. Zhao, C. C. Jiang, C. G. Hu, Z. L. Dong, J. L. Xue, Y. N. Meng, N. Zheng, P. W. Chen, L. T. Qu, *ACS Nano*,**2013**, *7*, 2406–2412.
7 H. H. Cheng,J. Liu, Y.Zhao,C. G. Hu, Z. P.Zhang, N.Chen,L. Jiang, L. T. Qu, *Angew. Chem. Int. Ed.*, **2013**, *52*, 10482–10486.
8 Y. H. Wang, K. Bian, C. G. Hu, Z. P. Zhang, N. Chen, H. M. Zhang, L. T. Qu, *Electrochem. Commun.*, **2013**, *35*, 49–52.
9 H. H. Cheng, Y. Hu, F. Zhao, Z. L. Dong, Y. H. Wang, N, Chen, Z. P. Zhang, L. T. Qu, *Adv. Mater.*,**2014,***26,* 2909–2913.
10 Z. B. Yang,H. Sun, T. Chen, L. B. Qiu, Y. F. Luo, H. S. Peng, *Angew. Chem. Int. Ed.*, **2013**. *52.* 7545–7548.
11 Y. N. Meng, Y. Zhao, C. G. Hu, H. H. Cheng, Y. Hu, Z. P. Zhang, G. Q. Shi, L. T. Qu, *Adv. Mater.*,**2013,***25,* 2326–2331.
12 Y. Y. Shang, X. D. He, Y. B. Li, L. H. Zhang, Z. Li, C. Y. Ji, E. Z. Shi, P. X. Li, K. Zhu, Q. Y. Peng, C. Wang, X. J. Zhang, R. G. Wang,J. Q. Wei, K. L. Wang, H. W. Zhu, D. H. Wu, A. Y. Cao,*Adv. Mater.*,**2012,***24,* 2896–2900.
13 M. W. Seto, B. Dick, M. J. Brett, *J. Micromech. Microeng.*, **2001,** *11,* 582–588.
14 J. T. Pham, J. Lawrence, D. Y. Lee, G. M. Grason, T. Emrick, A. J. Crosby, *Adv. Mater.*, **2013,** *25,* 6703–6708.
15 S. B. Smith, Y. Cui, C. Bustamante, *Science,* **1996,** *271,* 795–799.
16 D. J. Bell, L. Dong, B. J. Nelson, M. Golling, L. Zhang, D. Grützmacher, *Nano Lett.*, **2006,***6,* 725–729.
17 D. Grützmacher, L. Zhang, L. Dong, D. Bell, B. Nelson, A. Prinz, E. Ruh, *Microelectron. J.*, **2008,** *39,*478–481.
18 Z. P. Zeng, X. C. Gui, Z. Q. Lin, L. H. Zhang, Y. Jia, A. Y. Cao,Y. Zhu, R. Xiang, T. Z. Wu, Z. K. Tang, *Adv. Mater.*, **2013,** *25,* 1185–1191.
19 F. A. Hill, T. F. Havel, A. J. Hart, C. Livermore, *J. Micromech. Microeng.*, **2009,** *19.* 094015.
20 R. F. Zhang,Q. Wen, W. Z. Qian, D. S. Su, Q. Zhang, F. Wei, *Adv. Mater.*, **2011,** *23,* 3387–3391.
21 M. J. Madou, *Fundamentals of microfabrication: the science of miniaturization.* CRC press, **2002**.
22 P. X. Gao, W. J. Mai, Z. L. Wang, *Nano Lett.*, **2006,** *6,* 2536–2543.
23 A. E. Aliev, J. Y. Oh, M. E. Kozlov, A. A. Kuznetsov, S. L. Fang, A. F. Fonseca, R. Ovalle, M. D. Lima, M. H. Haque, Y. N. Gartstein, M. Zhang, A. A. Zakhidov, R. H. Baughman, *Science,* **2009,** *323,* 1575–1578.
24 R. Pelrine, R. Kornbluh, Q. Pei, J. Joseph, *Science,* **2000,** *287,*836–839.
25 J. D. W. Madden, N. A.Vandesteeg, P. A. Anquetil, P. G. A. Madden, A. Takshi, R. Z. Pytel, S. R. Lafontaine, P. A. Wieringa, I. W. Hunter, *IEEE J. Oceanic Eng.* **2004,** *29,* 706–728.

